IDENTIFICATION OF GENERALIZED VAN DER POL EQUATIONS FROM EXPERIMENTAL TIME SERIES OF ELECTRONIC NEURON

Lev Takaishvili
Peter the Great St. Petersburg
Polytechnic University
St.Petersburg, Russia
nar7187@yandex.ru

Vladimir Pomomarenko
Saratov Branch of Kotelnikov Institute of
Radio Engineering and Electronics of
Russian Academy of Sciences
Saratov, Russia
ponomarenkovi@gmail.com

Ilya Sysoev
Peter the Great St. Petersburg
Polytechnic University
St.Petersburg, Russia
ivssci@gmail.com

Article history:
Received 18.04.2026, Accepted 19.06.2026

Abstract

Currently, new electronic generators of neuron-like activity are being developed, which can be used both to build spike neural networks and, in the longer term, to solve the problems of neuroprosthetics and creation of artificial life. At the same time, the mathematical description of such artificial neurons is usually qualitative or fragmentary. Though writing equations from the first principles (e. g. from the Kirchhoff's laws) is still the main tool, there is another useful approach — system identification (model reconstruction) from experimental series. Actually, a combination of both approaches can give even more than each of them separately. The purpose of this work is to provide a new specific approach for identification of models which can to some extent be described by a generalized van der Pol oscillator. Since we propose this approach for a specific experimental device (electronic neuron) and test using its time series, we focused on some practical factors. First, we abandoned theoretical formulae for dissipation and potential functions and reconstructed them in the most general form without any additional assumptions. Second, we switched to equations integrated in time to reduce the impact of the measurement noise. Then, we considered the possibility of hysteresis for the dissipation function. Finally, we tested the approach based on series from three different instances of the same generator. We showed that the proposed approach can be useful to obtain the equations of the setup which really match the observed data.

Key words

model identification, van der Pol oscillator, electronic neuron, time series, nonlinear function

1 Introduction

Electronic models of neurons have been developed for last 35 years since the pioneering work [Mahowald and Douglas, 1991] by Mahowald and Douglas. Most of them have a mathematical description. Unfortunately, the real devices are usually described by the written equations very approximately. For example, the model [Binczak et al., 2003] is declared to be a hardware realization of FitzHugh–Nagumo neuron model, but the equations written in [Binczak et al., 2006] in detail do not match the experimental series well. The similar situation can be seen for electronic generators of neuron-like activity constructed by other principles. For instance, the phase-locked loop system proposed in [Shalfeev, 1968], found to be a good representative of neuron-like behavior in [Mishchenko et al., 2012] and realized in hardware in [Mishchenko et al., 2017] was then found to be described by the original equations with errors about 50% [Mishchenko et al., 2022], and its reconstructed nonlinear functions occurred very different from the expected ones. This problem usually arises because various approximations have to be used for the mathematical description of an experimental setup. For example, the diode is replaced with a nonlinear resistance or a parallel connection of resistance and capacitance, or it is assumed that the signal of the reference frequency generator is fully integrated (averaged).

Identification of system equations from experimental series is the most straightforward way to prove their compliance. This work aims to find out to what extent the equations derived in [Takaishvili et al., 2025] describe time series of the experimental generator presented there. Considering this problem in frames of the theory of reconstruction from time series [Gouesbet et al., 2003; Bezruchko and a. Smirnov, 2010] we may note that this is a "gray box" problem, where the

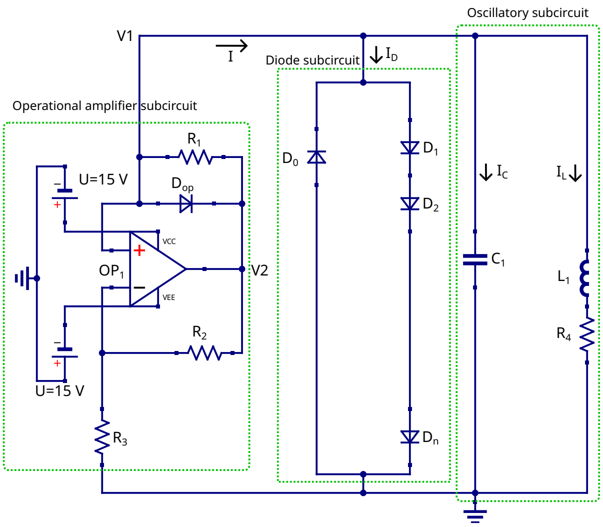

Figure 1. The considered circuit, where n is the number of diodes in the non-linear subcircuit.

model in general is known and the variables have some particular physical sense, but the nonlinear functions are unknown and have to be approximated. The considered model is a van der Pol oscillator with some general functions. Generalizations of van der Pol equations originally written for description of electronic oscillator [van der Pol, 1920] were fast found to be suitable for description of objects of very different nature [Van der Pol and van der Mark, 1928; Addoasah et al., 1995; Kovacic, 2011; Kuznetsov et al., 2014]. The state vector is two-dimensional and the voltage V_1 is considered as an observable. So, it is possible to reconstruct this vector by means of differentiation as it was proposed for more general models in [Gouesbet and Letellier, 1994] rather than using more difficult approaches to work with hidden variables [Baake et al., 1992] or the method of time delays [Packard et al., 1980].

2 The model and the task

In the study [Takaishvili et al., 2025] a new electronic generator of neuron-like activity was proposed and constructed, which can be described with the generalized van der Pol equation:

$$\frac{d^2V_1}{dt^2} + g(V_1)\frac{dV_1}{dt} + f(V_1) = 0, \tag{1}$$

where V_1 is the measurable voltage in the circuit (analog of transmembrane potential in the neuron), $g(V_1)$ is a nonlinear dissipation function, which also includes the source of energy (negative loss) provided by an operational amplifier, $f(V_1)$ is a significantly nonlinear potential function, with nonlinearity constructed using the diode subcircuit consisting of n_D diodes in one direction and a single diode in another (asymmetry was introduced to reduce the duty cycle). The diodes were considered as nonlinear conductivities; the diode capacitive properties being neglected at the working frequencies $\sim 10^4$ Hz.

In the paper [Takaishvili et al., 2025] the nonlinear functions f and g are written as follows:

$$f(V_1) = \frac{1 + (\rho + \rho_D)R_4}{L_1 C_1}, \tag{2}$$

$$g(V_1) = \frac{R_4}{L_1} + \frac{\rho + \rho_D}{C_1} + \frac{V_1}{C_1}\left(\frac{d\rho}{dV_1} + \frac{d\rho_D}{dV_1}\right), \tag{3}$$

where ρ is a conductivity of the operational amplifier subcircuit and ρ_D is a conductivity of the diode subcircuit, see Fig. 1. But the actual form of the functions $f(V_1)$ and $g(V_1)$ is the primary question. The analytical approximation for these functions was proposed in the original paper [Takaishvili et al., 2025]. These approximations use a non-ideal model for the operational amplifier and considers the diodes as nonlinear conductivity. Nevertheless, the straightforward use of these approximations for reconstruction from time series mostly failed even for the simplest case $n_D = 1$. In particular, only two parameters were identified with significant errors, different for different instances of the circuit. The underlying factors are as follows.

1. The used diodes were considered to be equal by their parameters and characteristics, but this is not the case, even for diodes of the same type and model from the same box.
2. Considering the diodes as nonlinear conductivity may be insufficient, or this conductivity function may significantly differ from the theoretical one.
3. The used model of operational amplifier is probably inadequate in the used regimes close to critical ones, but it is in these modes that the circuit works, generating high amplitude pulse activity.

The obvious way to solve all these problems is to abandon the direct analytical approximation of the functions $g(V_1)$ and $f(V_1)$. Instead, we propose to use implicit (table) function representation or decomposition of a function into a series

3 Method description

Here and further we suppose that the variable (voltage) V_1 from the equation (1) is measurable. We also suppose that this variable is the actual voltage in the studied setup, maybe with some possible measurement noise. Then, we decompose the function $f(V_1)$ in a Taylor's series, limited with K terms.

$$f(V_1) = \sum_{k=0}^{K} \alpha_k V_1^k, \tag{4}$$

where α_k are coefficients of decomposition.

In order to avoid decomposing $g(V_1)$ into a row too, let us partly follow the approach proposed in [Sysoev, 2018]. However, let us use it not literally, since the second derivative of the observable is very sensitive to the measurement noise, low sampling rate and insufficient discretization. To avoid these problems, at least partly, let us integrate the equation (1) over time:

$$\frac{dV_1}{dt} + \int g(V_1)\frac{dV_1}{dt}dt + \int f(V_1)dt = 0, \quad (5)$$

Let us then introduce a new unknown function $G(V_1)$ (antiderivative of the function $g(V_1)$):

$$\int g(V_1)\frac{dV_1}{dt}dt = \int g(V_1)dV = G(V_1),$$

with integration constant being a part of $G(V_1)$. Then, let us substitute the decomposition (4) into (5), resulting the following model, with moving the decomposition coefficients before the integration sign:

$$\frac{dV_1}{dt} + G(V_1) + \sum_{k=0}^{K} \alpha_k \int V_1^k dt = 0, \quad (6)$$

For convenience let us use the new notation:

$$\int V_1^k dt = \phi_k(t).$$

The series of ϕ_k can be calculated numerically from the observable. Note that the term at $k = 0$ is actually the integral of a constant by time, i. e. it may be written as $\alpha_0 t$ assuming that an integration constant is hidden in G. Let us denote $\frac{dV_1}{dt} = \dot{V}_1$ for simplicity and conciseness. Then, the time series $\dot{V}_1$ can be calculated numerically using Savitzky–Golay filter [Savitzky and Golay, 1964] (smoothing polynomial) is necessary. Next, we express $G(V_1)$ from the equation (6), given:

$$G(V) = -\dot{V} - \alpha_0 t - \sum_{k=1}^{K} \alpha_k \phi_k(t). \quad (7)$$

Since the values of V_1 are available only in the certain time points $t(n)$, where $n = 1, \dots, N$ are time point numbers of measurement, the formula (7) can be rewritten for specific time moments as follows:

$$G(V(n)) = -\dot{V}_1(n) - \alpha_0 t(n) - \sum_{k=1}^{K} \alpha_k \phi_k(n), \quad (8)$$

where $\phi_k(t_n)$ is denoted as $\phi_k(n)$ for brevity.

The function $G(V_1)$ is most likely continuous since it is an antiderivative of the function $g(V_1)$. This means that the close values of V_1 are mapped to the close values of G. Let us sort all observed values of $V_1(n)$ in ascending order, and denote as p_n the number of time point in the original (unsorted) time series such, that $V(n)$ is immediately followed by the value $V_1(p_n)$ in the sorted series. Due to continuity of the function $G(V_1)$ the difference between $V_1(n)$ and $V_1(p_n)$ is small if the time series length is large enough. Let us also state that the period of the measured time series and the measurement time step $\Delta t = t(n+1) - t(n) = 1/f_{\text{samp}}$ are in a rational ratio, where f_{samp} is a sampling rate of analog-digital converter. Additionally, if we consider the time series to be theoretically continuous and limited function of time, we obtain $\lim_{N\to\infty} |V_1(n) - V_1(p_n)| = 0$. It follows from the continuity of the function G that the value $\delta_n = G(V_1(n)) - G(V_1(p_n))$ is also a small value in modulus, and its limit at $N \to \infty$ is also 0. We use this property to construct the objective function, for which we will minimize the sum of the squares of the differences in the values of the function G corresponding to the neighboring values of the observable in the sorted series:

$$S(\vec{\alpha}) = \sum_{n=1}^{N} \delta_n^2, \quad (9)$$

where S is a function of a vector of parameters (coefficients) $\vec{\alpha} = (\alpha_0, \alpha_1, \dots, \alpha_K)$. It should also be noted that the terms for some numbers n fall out of the sum for technical reasons: those for which it is impossible to find the derivative numerically (last and first points of the series) and the value for which $p_n = N$. If the N is large enough, these losses are insignificant.

The formula (9) may be considered as a task for least squares approximation of the values $-(\dot{V}_1(n) - \dot{V}_1(p_n))$ using the functional basis set as $\phi_k(n) - \phi_k(p_n)$, with the zero-term of this basis being simply $t(n) - t(p_n)$. The solution of this task provides us with a set of α_k.

Practically, the proposed approach needs a correction. When calculating ϕ_k numerically, it is important to have a zero mean for $\overline{V_1^k}$. If $\overline{V^k} \neq 0$ the linear trend appears due to numerical integration in time. In absence of the trend for $k > 0$ the values of $\phi_k(n)$ and $\phi_k(p_n)$ would be close one to another due to the function is continuous and bounded; but due to the trend this is no more the case since $t(n)$ and $t(p_n)$ may be located very far in time, making the main impact into the differences $\big(\phi_k(n) - \phi_k(p_n)\big)$. To avoid this problem, let us introduce a new function $\varphi_k = \int (V_1^k - \overline{V_1^k})dt$. So,

$$\sum_{k=1}^{K} \alpha_k \phi_k = \sum_{k=1}^{K} \alpha_k \varphi_k - \sum_{k=1}^{K} \alpha_k \int \overline{V_1^k} dt. \quad (10)$$

Since all $\overline{V_1^k}$ are constants, the second term in the (10) is a linear trend which may be taken into account by correcting the α_0 coefficient. So, for the least squares routine replacing all ϕ_k by φ_k leads only to a corrected value of α_0 denoted further as $\tilde{\alpha}_0$. Therefore, the target function S takes the form (11):

$$S(\vec{\alpha}) = \sum_{n=1, p_n \neq N}^{N} \Big(-\big(\dot{V}_1(n) - \dot{V}_1(p_n)\big) - \tilde{\alpha}_0(t(n) - t(p_n)) - \sum_{k=1}^{K} \alpha_k \big(\varphi_k(n) - \varphi_k(p_n)\big) \Big)^2. \quad (11)$$

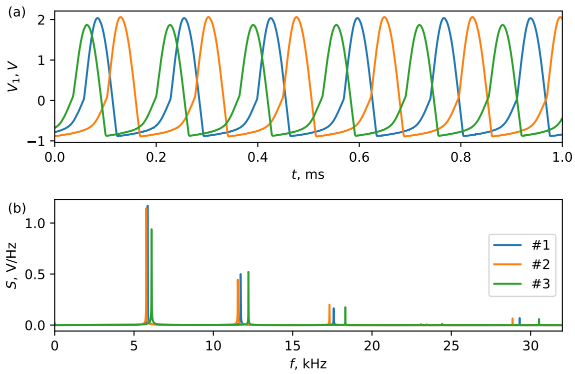

Figure 2. Time series (a) and amplitude spectra (b) for all three considered circuits in highly nonlinear regime with $R_2 = 1500\,\Omega$.

Here, we did not study in detail the question whether the constructed in this manner target function is asymptotically unbiased, i. e. whether the estimated values of $\vec{\alpha}$ tend to their true values for $N \to \infty$. We assume that all considerations from [Sysoev and Bezruchko, 2021] may be applied for the model (5). So, repeating similar arguments, we can conclude that, at least for some $g(V_1)$, we can rely on asymptotically unbiased estimates.

4 Devices, series and algorithms

In the paper [Takaishvili et al., 2025] the only experimental (hardware) circuit on the breadboard was considered together with SPICE simulation using Ngspice software [Madec M, 2017] and mathematical model. The characteristics of analog devices (diodes and an operational amplifier in our case) may differ for different instances, the results of reconstruction would be much more informative if several devices are considered. Therefore, we constructed three neurons same as in [Takaishvili et al., 2025] taking all components from the same box for maximal possible similarity, let us denote them “neuron #1”, #2 and #3 respectively.

For example, the time series of the observable V_1 for all three instances of the studied circuit in the highly nonlinear regime ($V_1 = 1500\ \Omega$) are plotted in the Fig. 2 (a). There is a visual difference in the oscillation amplitude: the third neuron has the amplitude notably lower then two others and the frequency — higher. The shape of oscillations is mostly the same for all three neurons (no visible difference), but the spectrum indicates some variations in power distribution between harmonics, see Fig. 2 (b). All signals are highly nonlinear with the power of the first harmonic being in the range 40–45% of the total signal power.

In the experiment, all time series of the observable V_1 were recorded with a professional 16-bit analogue-digital converter LCard E-502 at sampling rate of 2 MHz per channel. The series length was 0.1 s ($2 \cdot 10^5$ time points) with oscillation frequency being from ~ 10 kHz for quasi linear regimes ($R_2 = 600\ \Omega$) to ~ 5 kHz for highly nonlinear regimes ($R_2 = 1600\ \Omega$). Measurements were done for different R_2 from $R_2 = 600\ \Omega$ to $R_2 = 1600\ \Omega$ with the step of 50 Ω. Each of three neurons was measured independently. Only stable regimes were recorded and analyzed, transient processes were skipped.

Numerical differentiation was realized following [Savitzky and Golay, 1964]. Polynomials of the second order were constructed from $m = 11$ data point in the moving window, with the window central point corresponded to the time point where the derivative was calculated. For decomposition of the function f in a row different number of terms was considered. The approximation error depended on the K. Most results are reported for $K = 15$ which was considered to be large enough. Numerical integration was realized using Simpson’s second order method. For least squares, the routine `lstsq` from the `numpy.linalg` library was used [Virtanen et al., 2020].

The result of the proposed method application is a series of values of the function G for all used values of V_1 and the coefficients $\vec{\alpha}$. In addition, a relative approximation error may be calculated from the resulting value of the target function (9).

$$\varepsilon^2 = \frac{S(\vec{\alpha})}{\sigma_\delta^2 (N - (K+1) - (m-1))}, \qquad (12)$$

where $(N-(K+1))$ stays in the delimiter for effective number of independent values of δ_n. To reconstruct the dissipation function $g(V_1)$ we differentiated the resulting function $G(V_1)$ numerically, with V_1 sorted in ascending order. Note, that the resulting dependency $G(V_1)$ is obtained only for measured values of V_1 and is not equidistant by V_1, so we realized a general algorithm for smoothing with the second order polynomial and coefficients calculated by analytical formula (no numerical

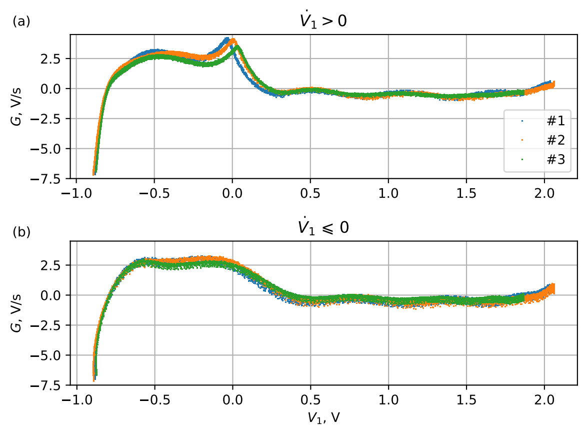

Figure 3. Results of reconstruction of functions $G_(V_1)$ for all three considered circuits in the highly nonlinear (spiking) regime with $R_2 = 1500\,\Omega$. Different colors are used for different instances. The upper subplot (a) corresponds to positive values of $\dot{V}_1$ and the lower subplot (b) — to non-negative ones. Since $G(V_1)$ includes unknown constant, the function mean was set to zero for plotting.

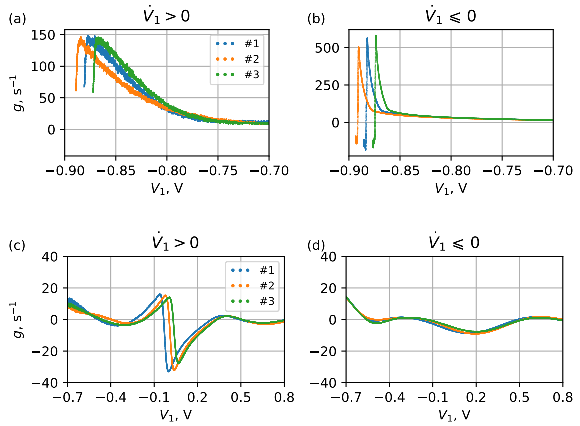

Figure 4. Reconstructed dissipation functions $g(V_1)$ for all three considered circuits in the highly nonlinear (spiking) regime with $R_2 = 1500\ \Omega$. Different colors are used for different instances. The subplot (a, c) correspond to positive values of $\dot V_1$ and the subplost (b, d) — to non-negative ones. The subplots (a, b) show only the dependency for the most negative values of $V_1 \in [-0.9; -0.7]$ V and the subplots correspond to the main range of $V_1 \in [-0.7; 0.8]$ V.

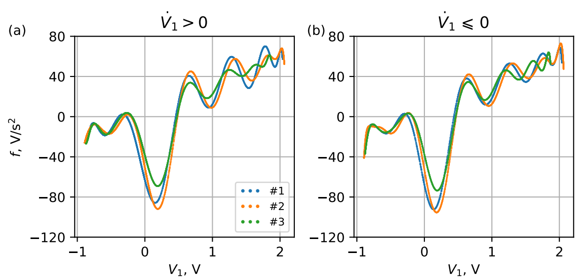

Figure 5. Reconstructed potential functions $f_(V_1)$ for all three considered circuits in the highly nonlinear (spiking) regime with $R_2 = 1500\ \Omega$. Different colors are used for different instances. The upper subplot (a) corresponds to positive values of $\dot V_1$ and the lower subplot (b) — to non-negative ones.

least squares routine was used here). To reconstruct the potential function $f(V_1)$ we used the reconstructed vector $\vec\alpha$ and simply calculated the values of $f(V_1)$ for all measured V_1 by the formula (4).

5 Results

When the proposed technique was applied, it turned out that the results in nonlinear regimes (when the diode D_{op} is open) significantly depend on the sign of $\dot V_1$. Most probably, this is a result of effects of D_{op} on the conductivity ρ. Mathematically, this can be explained by dependence of the dissipation function g on the term

$$\frac{d\rho}{dt} = \frac{d\rho}{dV_1}\frac{dV_1}{dt}.$$

It looks like ρ is a function of $\dot V_1$ is some sense. To manage this problem we performed reconstruction differently for $\dot V_1 > 0$ and $\dot V_1 \leqslant 0$.

The results of reconstruction of the function $G(V_1)$ in the highly nonlinear mode ($R_2 = 1500\ \Omega$) using the polynomial order $K = 15$ are presented in Fig. 3. Different colors indicate the functions reconstructed for different neurons separately for $\dot V_1 > 0$, see Fig. 3 (a), and for $\dot V_1 \leqslant 0$, see Fig. 3 (b). The resulting dependencies obviously indicate qualitative difference between functions reconstructed for positive and negative values of $\dot V_1$. At the same time, the curves corresponding to different neurons are qualitatively similar. In particular, for positive values of $\dot V_1$ one can see a global maximum at $V_1 \approx 0$ V and local minimum at $V_1 \approx -0.2$ V. All the dependencies for $V_1 > 0.5$ V are very similar and have the oscillatory "tail" due to polynomial approximation of $f(V_1)$. It is essential that the curves for $\dot V_1 > 0$ and for $\dot V_1 \leqslant 0$ differ mainly when the current flows through the diode $D_{\rm op}$.

The dissipation function $g(V_1)$ was reconstructed by means of numerical differentiation of the reconstructed function $G(V_1)$. To investigate the actual behavior of the $g(V_1)$, let us split the plot into two parts. This is necessary since the function values are very different at the beginning, where $G(V_1)$ changes fast (note, that $g(V_1)$ is its derivative), and further. First, let us consider a small range for lowest values of $V_1 \in [-0.9; -0.7]$ V.

At the most negative values of V_1 the curves for different instances look similar but not completely identic, see Fig. 4 (a, b). The dependencies for the positive and non-negative values of $\dot V_1$ also look different, see Fig. 4 (c, d). The maximal values for $\dot V_1 \leqslant 0$ are three times larger, but the dependency approaches zero faster. This fundamental difference in $g(V_1)$ values actually prevents fine reconstruction without splitting the measured series by the sign of $\dot V_1$.

The reconstructed potential functions are very similar for different conditions: $\dot V_1 > 0$ and for $\dot V_1 \leqslant 0$ — compare subplots (a) and (b) of Fig. 5. This indicates the critical role of approximation of $g(V_1)$ in success of the reconstruction algorithm. The reconstructed for different neurons functions $f(V_1)$ generally look like a negative Gaussian with a linear trend. Large oscillations are the result of polynomial decomposition (4).

6 Conclusion

In this paper we present a novel approach to reconstruction of a generalized van der Pol oscillator equations from scalar time series, then we used this approach to reconstruct the model of electronic neuron. The approach was adapted for series from experimental setups by means of implementing the following ideas.

- The oscillator is reconstructed in the general form without explicit approximation of both dissipation and potential functions.
- To reduce the measurement noise impact the equations are reconstructed in the form after integration by time.

- The target function is constructed as a length (in some sense) of the antiderivative of the dissipation function, so, this antiderivative is obtained in the table form (no approximation is necessary, as well as no decomposition in a row).
- It is possible to split the series by any condition, for instance, by the sign of the derivative of the observable, and perform the reconstruction separately for different values of the condition.

By this way, the proposed approach occurs to be very flexible, which is necessary for experimental data, where the theoretically proposed model often does not fit the actual evolution operator well [Mishchenko et al., 2012].

Identification of models for electronic generators of neuron-like activity is a fundamental task necessary to be solved for the practical implementation of these models. Unfortunately, most neuron models proposed so far from the very beginning [Mahowald and Douglas, 1991; Rasche and Douglas, 2000; Pinto et al., 2000] are still modelled only from the first principles, i. e. the equations are written from Kirchhoff's laws with some limitations and approximations, but their relevance was never tested quantitatively. This problem is mostly relevant for the models which rely on semiconductor devices those nonlinear conductivity and capacity are considered to be theoretically known (it would be possible to use vacuum devices instead of semiconductor ones, but we do not know any implementation of electronic neurons based on such elements). While generally this approach works and the resulting generators are able to produce the spiking (and sometimes bursting, see e. g. [Mishchenko et al., 2012]) behavior, there is no evidence to what extent the written mathematical models match the experimental setup. This also makes a large problem of interpretation of the bifurcation analysis performed for such models theoretically (very popular approach in recent years, see [Basu et al., 2010; Bao et al., 2019; Zhang et al., 2023] for instance): it demands straightforward repetition in the hardware experiment.

We started to reduce this gap between the experimental setups and corresponding models from the neuron we have proposed recently in [Takaishvili et al., 2025]. To study the problem in detail we constructed three instances of the generator and compared the results between them: this helps to understand how much the possible variance of setup parameters natural for any hardware realization effects the model. It also occurred that the model matches the data significantly better when considering the task separately for positive and negative values of the observable derivative: in the considered case the piecewise approximation decreased the relative approximation error by ~ 1.8 times.

We found that the antiderivative of the dissipation function (designed as G in this paper) has a specific form similar to all three considered instances. We suppose that in some future work a good candidate for explicit approximation can be found, especially for $\dot{V}_1 \leqslant 0$. To find it, a lasso-like approach may be used [Kukreja et al., 2006; Casadiego et al., 2017].

We think that the proposed technique can be applied to some other electronic neuron generators as well as to different objects which may be to some extent described by the generalized van der Pol equations. In particular applications to biological objects where van der Pol like models were already in use look promising [Stoop et al., 2006]. The approach can be also applied to other systems, for example, neural mass models as proposed by [Plotnikov, 2024], if we consider that every second variable (all even or all odd) is measurable (the other variables may be reconstructed by means of numerical differentiation or integration). another possible extension of the proposed approach is for regularly driven oscillators. This problem was partly solved in [Besruchko and Smirnov, 2000; Smirnov et al., 2003], but the robustness of the noise in the cited papers is insufficient to many real world applications like considered in [Ivanov et al., 2024] due to necessity to calculate numerically the second derivative. Yet another application may be considered for subnetworks of the systems described by equations of the first order, see [Kashchenko, 2026]. E. g. if we consider two last elements of the chain from [Kashchenko, 2026], we can see that their dynamics together may be rewritten as a second order van der Pol like equation.

7 Acknowledgements

The research was supported by Russian Science Foundation, Russia (project No. 25-12-00176, `https://rscf.ru/project/25-12-00176/`).

References

Addoasah, W., Akpati, H., and Mickens, R. (1995). Investigation of a generalized van der Pol oscillator differential-equation. *Journal of Sound and Vibration*, **179** (4), pp. 733–735.

Baake, E., Baake, M., Bock, H., and Briggs, K. (1992). Fitting ordinary differential equations to chaotic data. *Phys. Rev. A*, **45** (8), pp. 5524–5529.

Bao, H., Hu, A., Liu, W., and Bao, B. (2019). Hidden bursting firings and bifurcation mechanisms in memristive neuron model with threshold electromagnetic induction. *IEEE transactions on neural networks and learning systems*, **31** (2), pp. 502–511.

Basu, A., Petre, C., and Hasler, P. E. (2010). Dynamics and bifurcations in a silicon neuron. *IEEE Transactions on Biomedical Circuits and Systems*, **4** (5), pp. 320–328.

Besruchko, B. P. and Smirnov, D. A. (2000). Constructing nonautonomous differential equations from experimental time series. *Phys. Rev. E*, **63**, pp. 016207.

Bezruchko, B. P. and a. Smirnov, D. (2010). *Extracting Knowledge From Time Series: (An Introduction to Nonlinear Empirical Modeling)*. Springer Series in Synergetics. Springer, New York.

Binczak, S., Jacquir, S., Bilbault, J.-M., Kazantsev, V. B., and Nekorkin, V. I. (2006). Experimental study of electrical FitzHugh–Nagumo neurons with modified excitability. *Neural Networks*, **19** (5), pp. 684–693.

Binczak, S., Kazantsev, V. B., Nekorkin, V. I., and Bilbault, J. M. (2003). Experimental study of bifurcations in modified FitzHugh–Nagumo cell. *Electronics Letters*, **39** (13), pp. 1.

Casadiego, J., Nitzan, M., Hallerberg, S., and Timme, M. (2017). Model-free inference of direct network interactions from nonlinear collective dynamics. *Nature Communications*, **8**, pp. 2192.

Gouesbet, G. and Letellier, C. (1994). Global vector-field reconstruction by using a multivariate polynomial l2 approximation on nets. *Phys. Rev. E*, **49**, pp. 4955.

Gouesbet, G., Meunier-Guttin-Cluzel, G., and Menard, O. (2003). *Chaos and its Reconstruction*. Nova Science Publishers, New York.

Ivanov, D., Zhdanov, A., and Sandler, I. (2024). Identification of dynamical systems with time-varying disturbances and fractional errors-in-variables. Application example to a drone model. *Cybernetics and Physics*, **13** (1), pp. 49–56.

Kashchenko, S. A. (2026). Local dynamics of aperiodic chains with unidirectional couplings. *Izvestiya VUZ. Applied Nonlinear Dynamics*, **34** (1), pp. 9–33.

Kovacic, I. (2011). On the motion of a generalized van der Pol oscillator. *Communications in Nonlinear Science and Numerical Simulation*, **16** (3), pp. 1640–1649.

Kukreja, S. L., Löfberg, J., and Brenner, M. J. (2006). A least absolute shrinkage and selection operator (lasso) for nonlinear system identification. *IFAC proceedings volumes*, **39** (1), pp. 814–819.

Kuznetsov, A. P., Seliverstova, E. S., Trubetskov, D. I., and Turukina, L. V. (2014). Phenomenon of the Van der Pol equation. *Izvestiya VUZ. Applied Nonlinear Dynamics*, **22** (4), pp. 3–42.

Madec M, Lallement C, H. J. (2017). Modeling and simulation of biological systems using spice language. *PLOS ONE*, **12** (8).

Mahowald, M. and Douglas, R. (1991). A silicon neuron. *Nature*, **354**, pp. 515–518.

Mishchenko, M. A., Bolshakov, D. I., and Matrosov, V. (2017). Instrumental implementation of a neuronlike generator with spiking and bursting dynamics based on a phase-locked loop. *Tech. Phys. Lett.*, **43**, pp. 596–599.

Mishchenko, M. A., Bolshakov, D. I., Vasin, A. S., Matrosov, V. V., and Sysoev, I. V. (2022). Identification of phase-locked loop system from its experimental time series. *IEEE Transactions on Circuits and Systems II: Express Briefs*, **69** (3), pp. 854–858.

Mishchenko, M. A., Shalfeev, V. D., and Matrosov, V. V. (2012). Neuron-like dynamics in phase-locked loop. *Izvestiya VUZ. Applied Nonlinear Dynamics*, **20** (4), pp. 122–130.

Packard, N. H., Crutchfield, J. P., Farmer, J. D., and Shaw, R. S. (1980). Geometry from a time series. *Physical review letters*, **45** (9), pp. 712.

Pinto, R. D., Varona, P., Volkovskii, A., Szücs, A., Abarbanel, H. D., and Rabinovich, M. I. (2000). Synchronous behavior of two coupled electronic neurons. *Physical Review E*, **62** (2), pp. 2644.

Plotnikov, S. A. (2024). Identification of neural mass network parameters using eeg evoked potential data. *Cybernetics and Physics*, **13** (4), pp. 296–301.

Rasche, C. and Douglas, R. (2000). An improved silicon neuron. *Analog Integrated Circuits and Signal Processing*, **23**, pp. 227–236.

Savitzky, A. and Golay, M. (1964). Smoothing and differentiation of data by simplified least squares procedures. *Analytical Chemistry*, **38** (8), pp. 1627–1639.

Shalfeev, V. D. (1968). Investigation of the dynamics of a system of automatic phase control of frequency with a coupling capacitor in the control loop. *Radiophys Quantum Electron*, **11** (3), pp. 221–226.

Smirnov, D. A., Sysoev, I. V., Seleznev, E. P., and Bezruchko, B. P. (2003). Global reconstruction from nonstationary data. *Technical Physics Lett.*, **29** (10), pp. 824–827.

Stoop, R., Kern, A., Göpfert, M. C., Smirnov, D., Dikanev, T., and Bezrucko, B. (2006). A generalization of the van-der-Pol oscillator underlies active signal amplification in Drosophila hearing. *European Biophysics Journal*, **35** (6), pp. 511–516.

Sysoev, I. V. (2018). Reconstruction of ensembles of generalized van der pol oscillators from vector time series. *Physica D: Nonlinear Phenomena*, **384–385**, pp. 1–11.

Sysoev, I. V. and Bezruchko, B. P. (2021). Noise robust approach to reconstruction of van der Pol-like oscillators and its application to Granger causality. *Chaos*, **31**, pp. 083118.

Takaishvili, L. V., Ponomarenko, V. I., and Sysoev, I. V. (2025). Simple tunable generator of neuron-like activity. *Chaos, Solitons & Fractals*, **196**, pp. 116316.

van der Pol, B. (1920). A theory of the amplitude of free and forced triode vibrations. *Radio Review (later Wireless World)*, **1**, pp. 701–710.

Van der Pol, B. and van der Mark, J. (1928). The heartbeat considered as a relaxation oscillation, and an electrical model of the heart. *Philosophical Magazine & Journal of Science*, **6** (38), pp. 763.

Virtanen, P., Gommers, R., Oliphant, T. E., Haberland, M., Reddy, T., Cournapeau, D., Burovski, E., Peterson, P., Weckesser, W., Bright, J., et al. (2020). Scipy 1.0: fundamental algorithms for scientific computing in python. *Nature methods*, **17** (3), pp. 261–272.

Zhang, X., Min, F., Dou, Y., and Xu, Y. (2023). Bifurcation analysis of a modified fitzhugh-nagumo neuron with electric field. *Chaos, Solitons & Fractals*, **170**, pp. 113415.